7 Model Validation and Base Simulations

The hydrodynamic and sediment transport components of the model were validated by comparison to field measurements compiled from a number of sources. A model mesh was developed to describe the geometry, frictional, and seagrass conditions over the system. Time-series tidal, wind, and freshwater inflows were compiled and used to force the model on its boundaries. The model was operated and adjusted until agreement with available hydrodynamic and suspended sediment field data was deemed satisfactory. The model was then used in annual base simulations for no-disposal and six-disposal scenarios. Two sets of model-to-prototype comparisons were made for TSM, channel shoaling, and PA sediment dispersion. The technical issue is whether or not resuspended dredged material limits the growth, survival, and re-establishment of seagrass by limiting the availability of light to the macrophtes. Seagrass limits resuspension, and suspended sediment concentrations are generally low in seagrass areas.

Model Mesh

Depths for the model mesh were obtained from a survey performed by John Chance & Associates under contract to CESWG in 1995. The survey covered the entire system, including tidal flats to +0.6 m mean lower low water (mllw). The Surface-water Modeling System (SMS©, Brigham Young University 1997) was used to develop the model mesh, specify material types and display results. The model mesh included Lower and Upper Laguna Madre, South Bay, Baffin Bay, and the GIWW, including the Land Cut. The tidal boundaries were located outside the system: north of the J. K. Kennedy Causeway in Corpus Christi Bay, and east of Port Mansfield and Brazos Santiago Passes.

The model mesh describing the geometry of the system consisted of about 20,000 nodes. Node locations and mesh bathymetry are shown in Figures 73, 74, and 75 along with the locations of the TNRCC monitoring stations. The mesh had highest resolution generally near the Lower Laguna Madre navigation channel and around disposal areas and near the mouth of Baffin Bay in Upper Laguna Madre. Element size varied. For example, in the GIWW mesh elements were 38.1 m (125 ft) wide, while those at the other extreme had sides on the order of a kilometer.

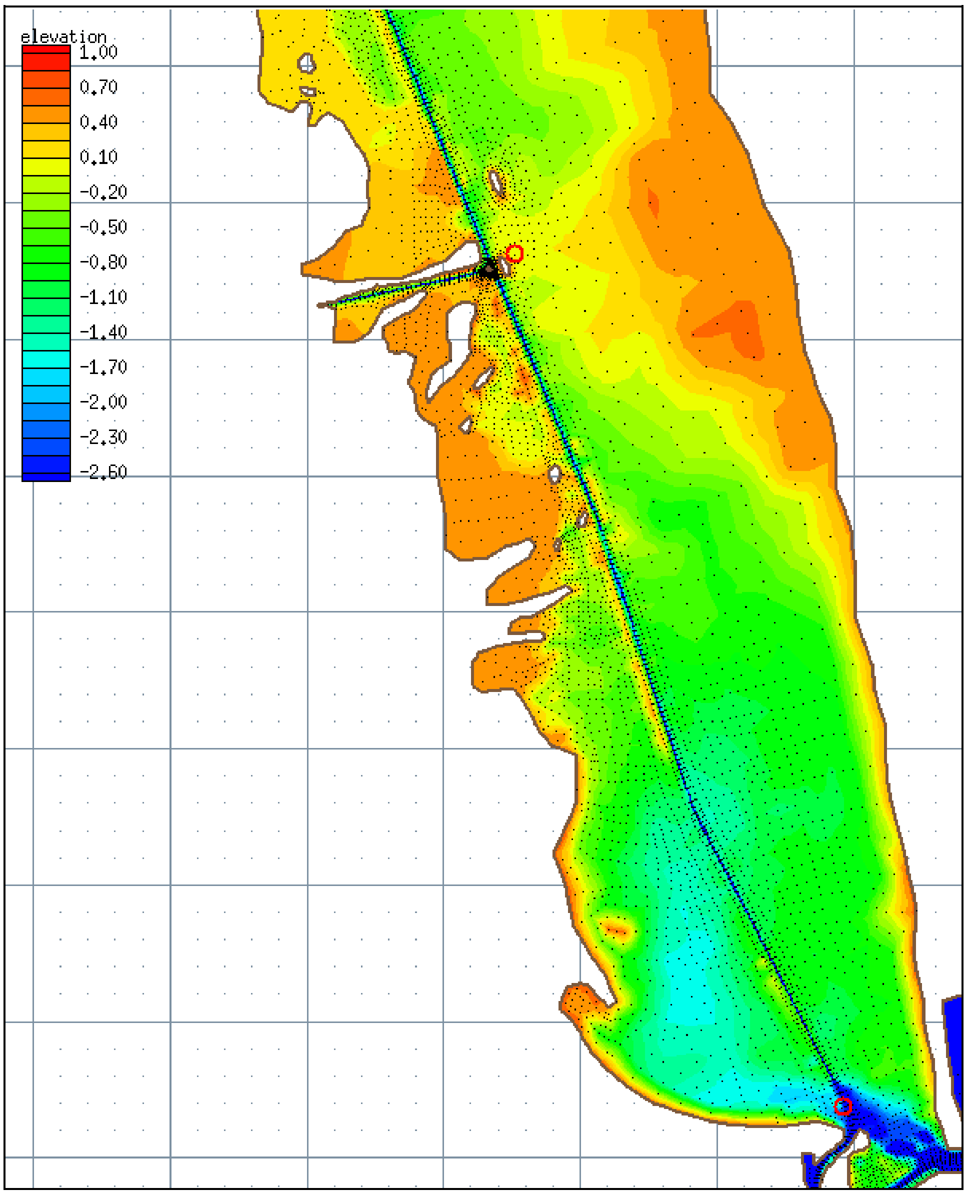

Figure 73. Model mesh nodes and depths. TNRCC stations TNR-446 and TNR-447 are indicated as circles south-to-north along the GIWW

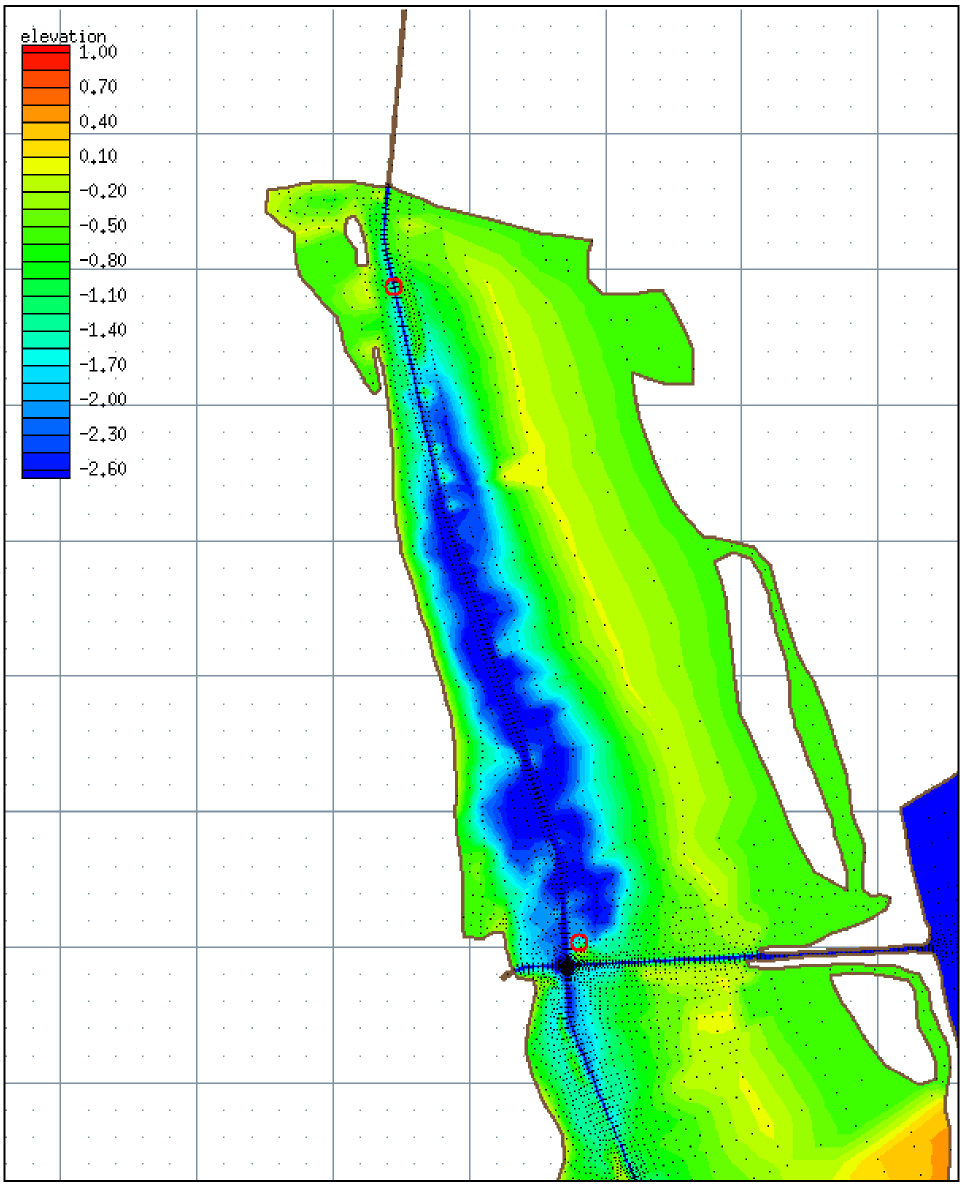

Figure 74. Model mesh nodes and depths. TNRCC stations TNR-448 and TNR-449 are indicated as circles south-to-north along the GIWW

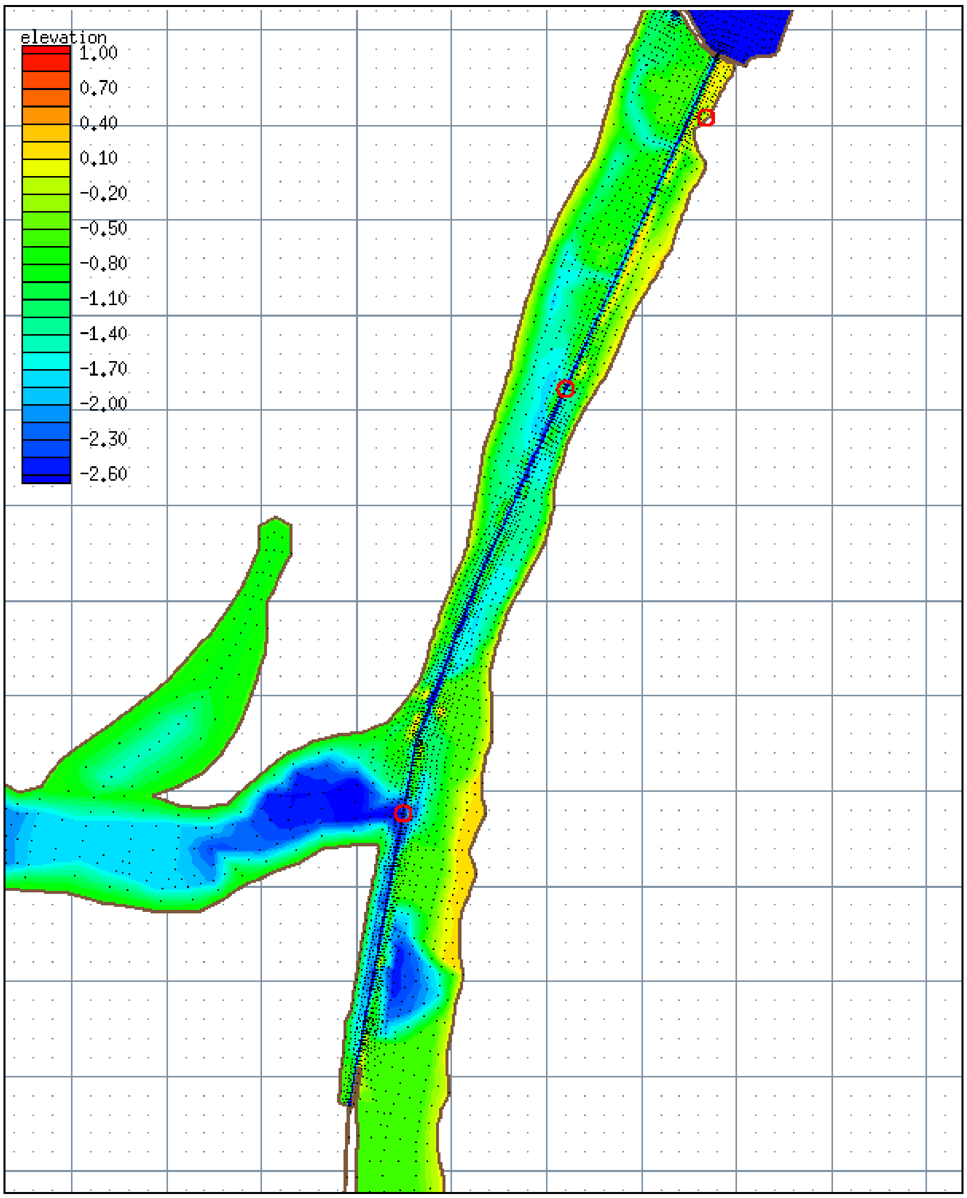

Figure 75. Model mesh nodes and depths. TNRCC stations TNR-444, -445, and -443 are indicated as circles south-to-north along the GIWW

Part of the model mesh development included specifying bottom material types. Bed-material types were used in specifying bed-frictional characteristics, sediment grain-classes, and vertical bed-density structures, which control the transport conditions for deposited materials. For this study, material types were given special consideration, and model enhancement included the local specification of atmospheric-drag coefficient, and seagrass sheltering of the bed from hydraulic shear stress. Background information on the friction and bed-sheltering characteristics of seagrass are presented in Chapter 6.

Seagrasses were specified by *Thalassia*, *Syringodium*, and *Haladule* species according to distribution information from White et al. (1986 and 1989), Onuf (1979), and Brown and Kraus (1997). Grain-size bed indices were developed from the maps presented by White et al. (1986 and 1989). The union of seagrass species, bare, and reef-bed coverage with grain-size index were used to specify the model bed-material types as shown in Figures 76 and 77.

Hydrodynamic Model Validation

Initial rough adjustments of the model were based on a June 1991 data set that emphasized Upper Laguna Madre. The main data set used for model validation was collected in June 1997 and emphasized Lower Laguna Madre. Both data sets were collected by the Texas Water Development Board in cooperation with the U. S. Geological Survey and CBI. Measured tidal discharges, current velocities, and water levels were compared to the model.

The model was operated with freshwater inflow at Arroyo Colorado, wind stress, evaporation, and tidal head boundaries. At Arroyo Colorado, an average, constant freshwater inflow of 14.2 m^3/sec was specified in the model (White et al. 1986 and 1989). An evaporative loss of 71.1 cm/yr over and above an annual average rainfall of 63.5 cm/yr (White et al. 1986 and 1989) was specified in the model as a constant value uniformly over the mesh.

Validation data set

Wind- and water-level data used to develop model boundary conditions were obtained from the CBI's Texas Coastal Ocean Observation Network (TCOON) web site. Wind data for the June 1997 validation period were compiled from a station at Port Mansfield. (Wind data from South Padre Island and the Naval Air Stations had many missing readings and were not used for this time period.) Hourly winds were low-pass filtered to remove fluctuations shorter than a period of about three hours. This filtering was accomplished by application of a local running least-squares smoother. Smoothed wind data were then linearly interpolated to one-hour intervals, which replaced 99 missing reading.

Water level data were compiled from Bob Hall Pier (maintained by NOAA) and Packery Channel (maintained by CBI). The tidal signals were low-pass filtered as previously described. The Bob Hall tidal signal was applied without any amplitude or phase adjustment to the Mansfield and Brazos ocean boundaries. Reasonable tidal signals at Port Mansfield and South Padre Island were produced. The Packery Channel tidal signal was applied to the Corpus Christi Bay boundary

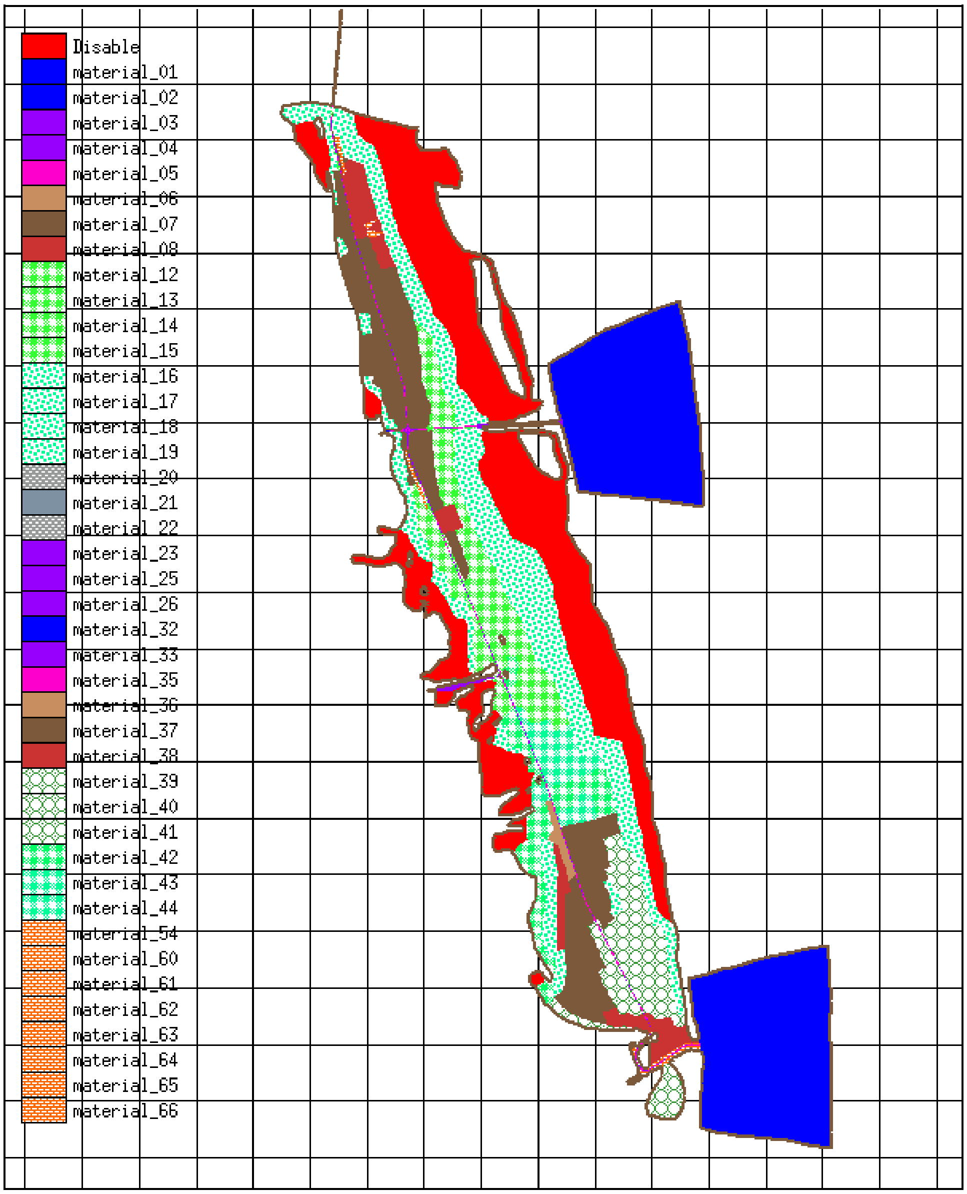

Figure 76. Lower Laguna Madre model bed material types. Bare areas are solid colors and seagrass areas are textured green colors

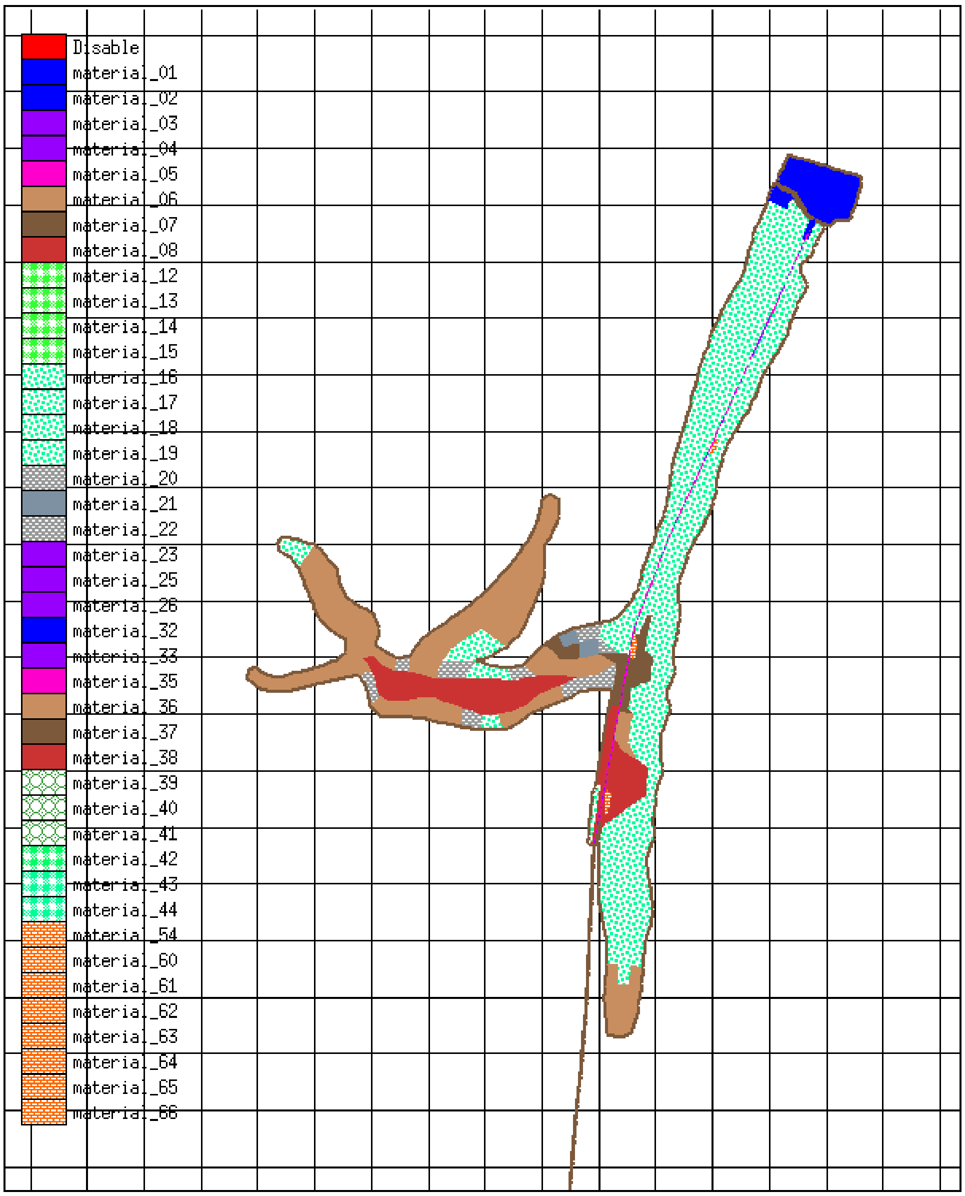

Figure 77. Upper Laguna Madre model bed material types. Bare areas are solid colors and seagrass areas are textured green colors

of the model. The model was operated for the period 22 May to 22 June 1997, and model results compared to field data.

Model-prototype comparisons

Water-surface elevations comparisons at eight stations for the 1997 validation period are shown in Figure 78a and b. Tidal water surface elevations are generally the easiest parameter to adjust in a hydrodynamic model. In the case of Laguna Madre, tidal ranges are small, and phase and amplitude changes and wind effects are large.

The 1998 wave data described in Chapter 2 was used to perform an additional check on model water levels. Mean water-surface elevations were extracted from the pressure signal recorded by wave gauges at L1w and L2w (located at LLM1 and LLM2a). Data at the South Padre Island (SPI) tide station, representing the tidal input for this area, were downloaded from the CBI TCOON website for this time period. Model data were extracted for an available time period that appeared to have similar tidal characteristics at SPI. Standard deviations (σ) were computed for the field and model water-level data for a period of 19 days. Results, and results normalized by the SPI value, are shown in Table 35. The model reproduced the considerable change in tidal amplitude that occurs north of Port Isabel.

Table 35
Field and Model Tidal Water Level Variability for January 1998

	4 σ, m		Ratio with SPI	
Station	Field	Model	Field	Model
SPI	0.64	0.72	1.00	1.00
L1w	0.35	0.38	0.55	0.53
L2w	0.39	0.43	0.61	0.59

Model and field tidal discharges are shown in Figures 79 to 83 for the five tidal discharge ranges. Comparisons of tidal discharges across passes and inlets check the model’s tidal prism.

Plots of model versus field current magnitudes at four stations are shown in Figure 84. These comparisons check the model’s ability to reproduce currents, but comparisons are sensitive to gauge location, especially around small-scale channel or other geometric features. Model currents at South Bay and Port Isabel were much lower than field values, even though tidal discharges at these locations were only slightly lower than field values. In other words, general currents were predicted by the model better than currents at particular points. Model currents at Lower Laguna Madre West of the GIWW and at Arroyo Colorado stations were about equivalent to or greater than field currents. In the case of Lower Laguna Madre West of the GIWW, examination of the electromagnetic current meter data

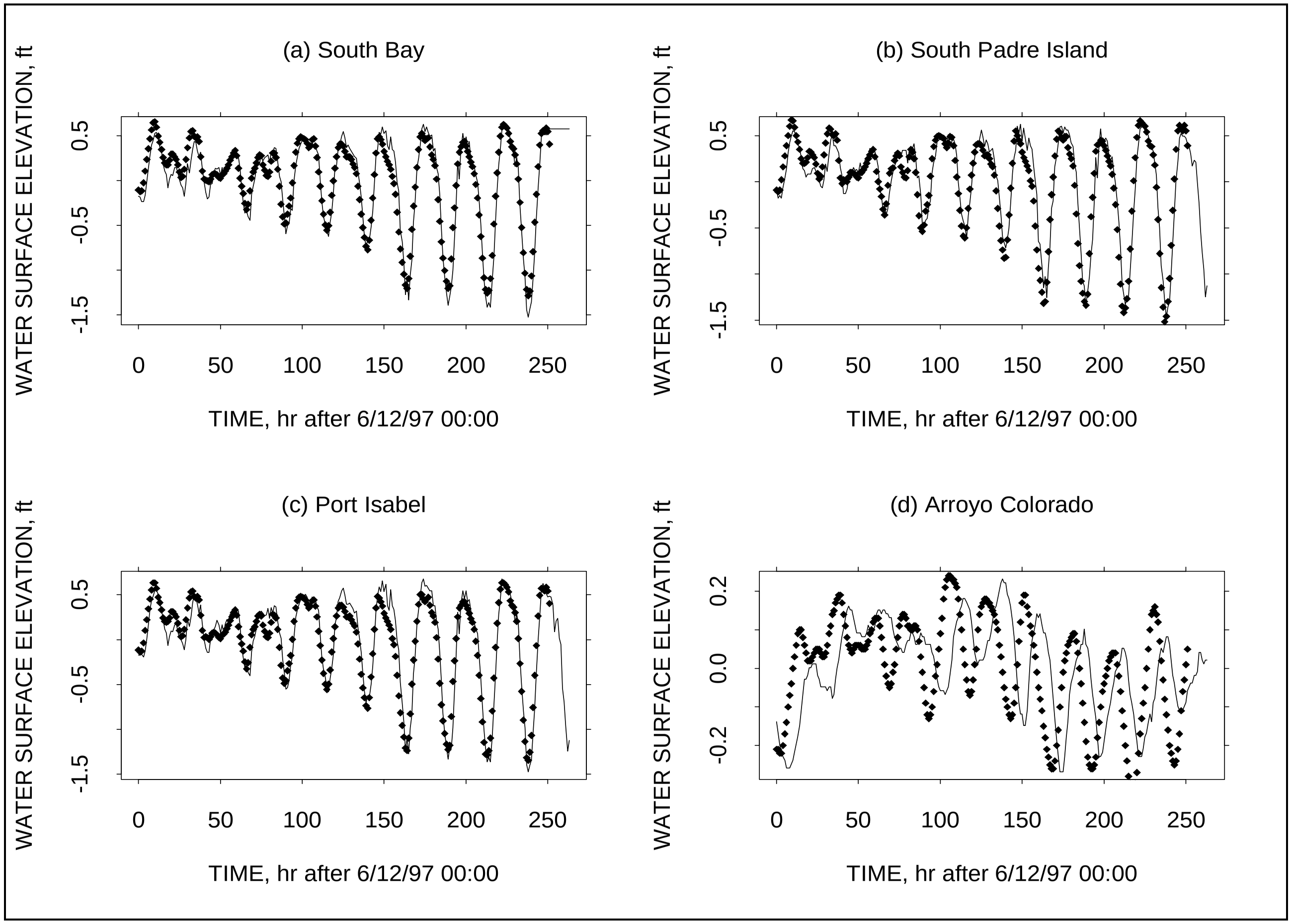

Figure 78a. Model and prototype 1997 water-surface elevation comparisons

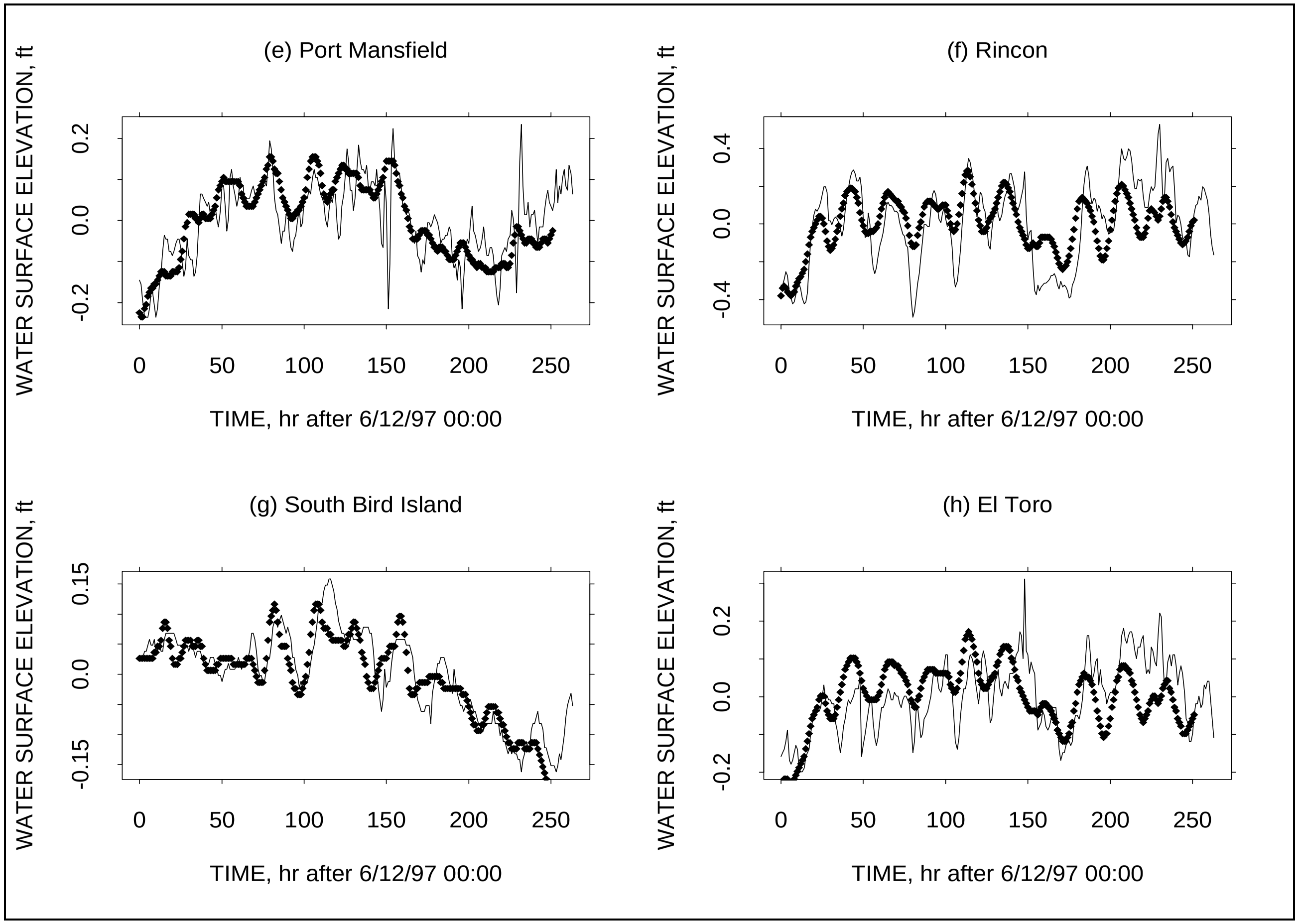

Figure 78b. Model and prototype 1997 water-surface elevation comparisons

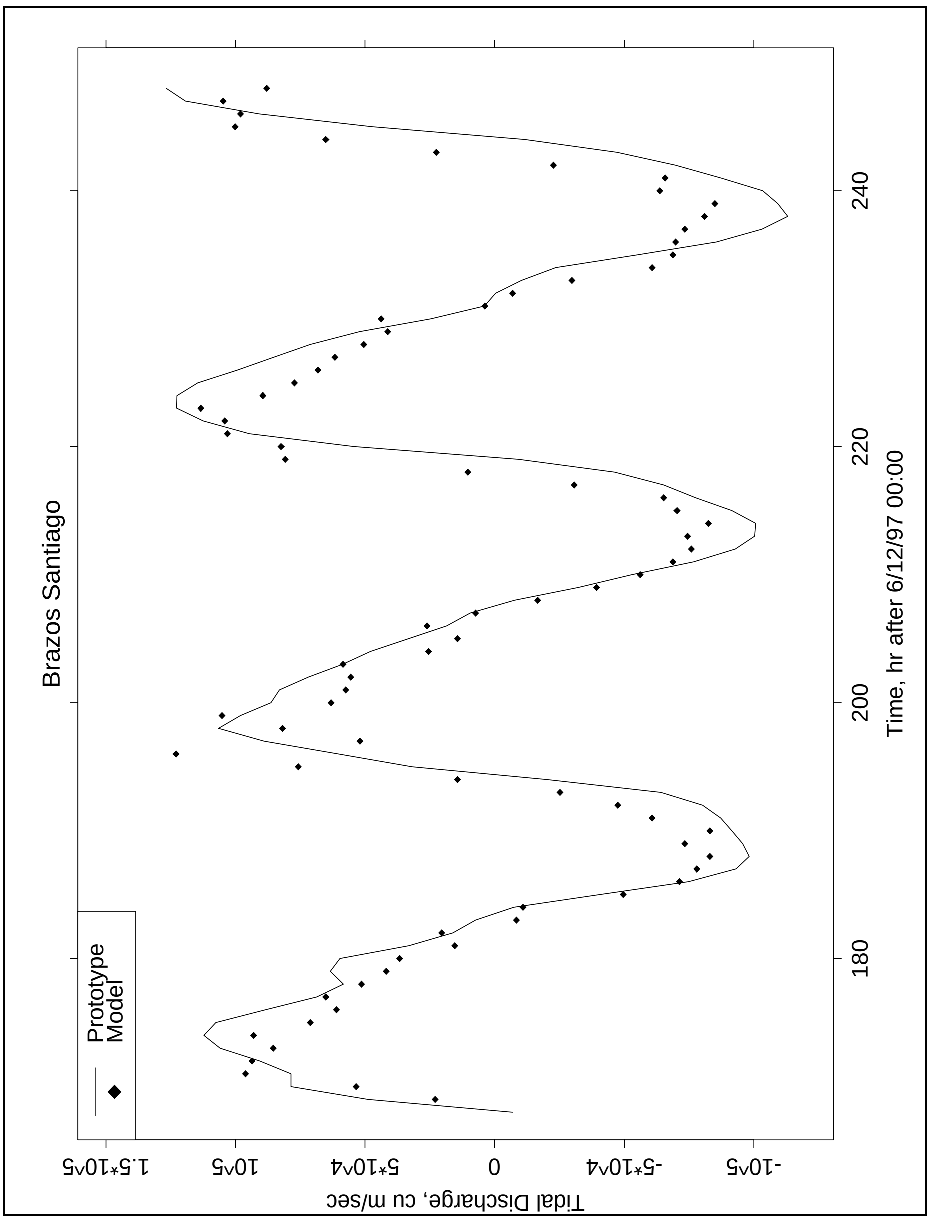

Figure 79. Model and prototype tidal discharges at Brazos Santiago

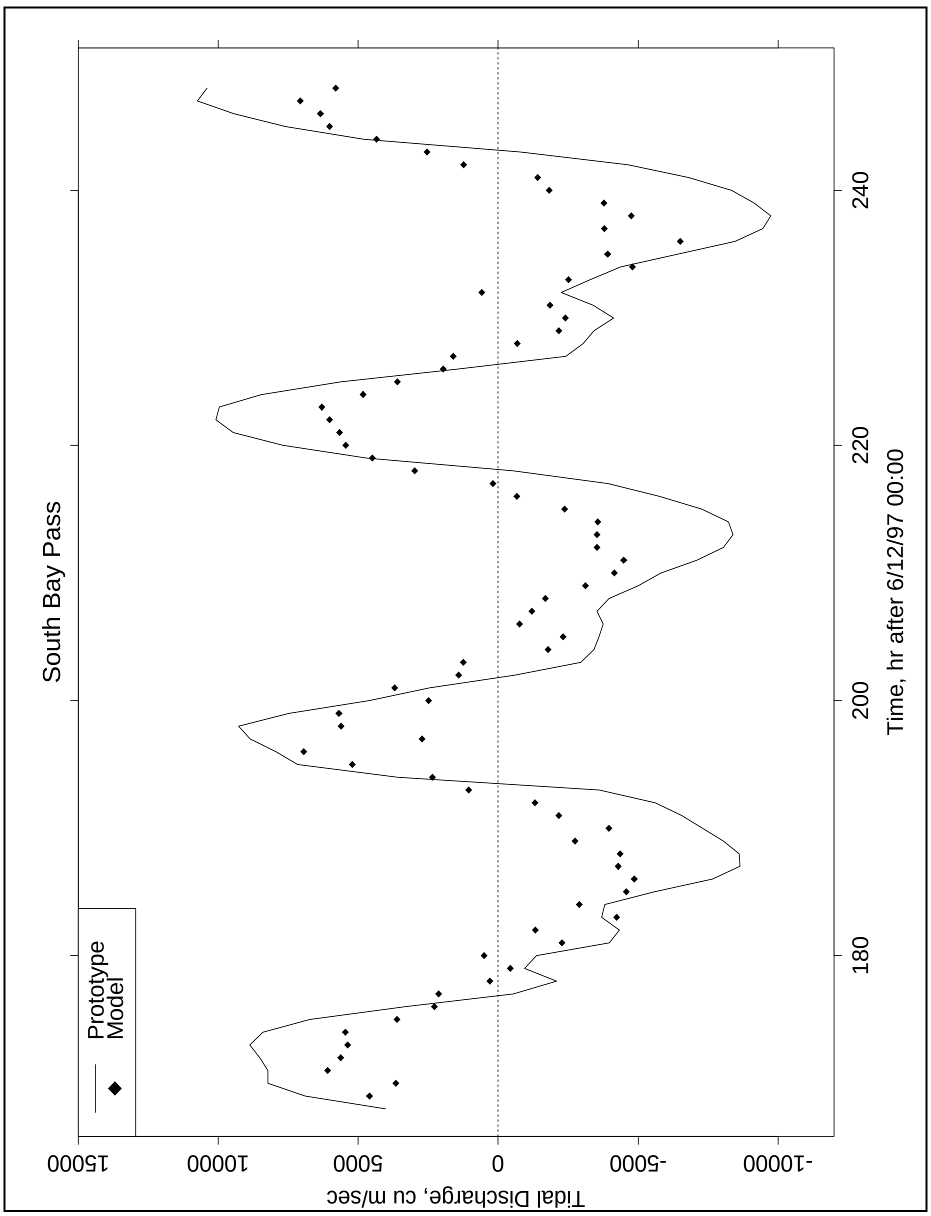

Figure 80. Model and prototype tidal discharges at South Bay Pass

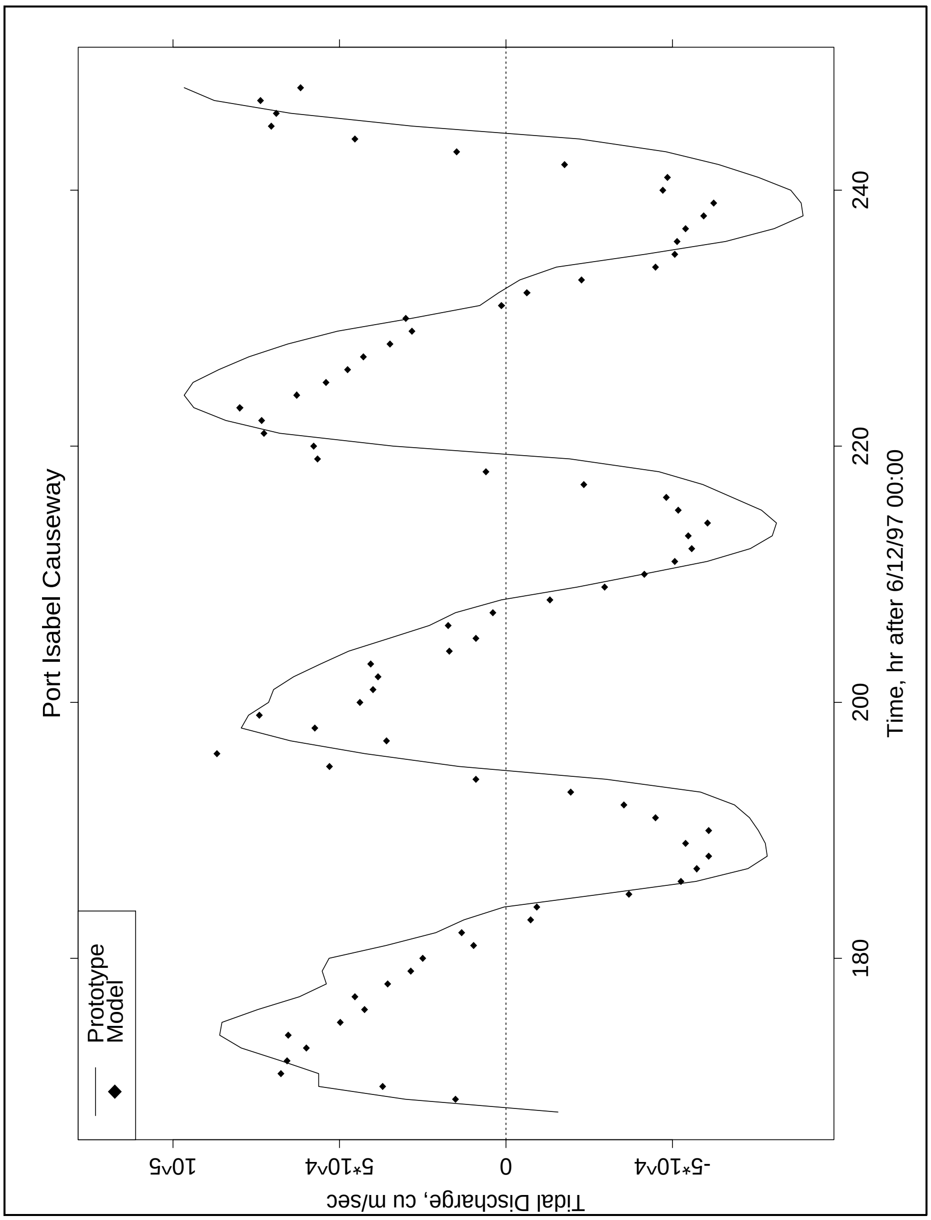

Figure 81. Model and prototype tidal discharges at Port Isabel Causeway

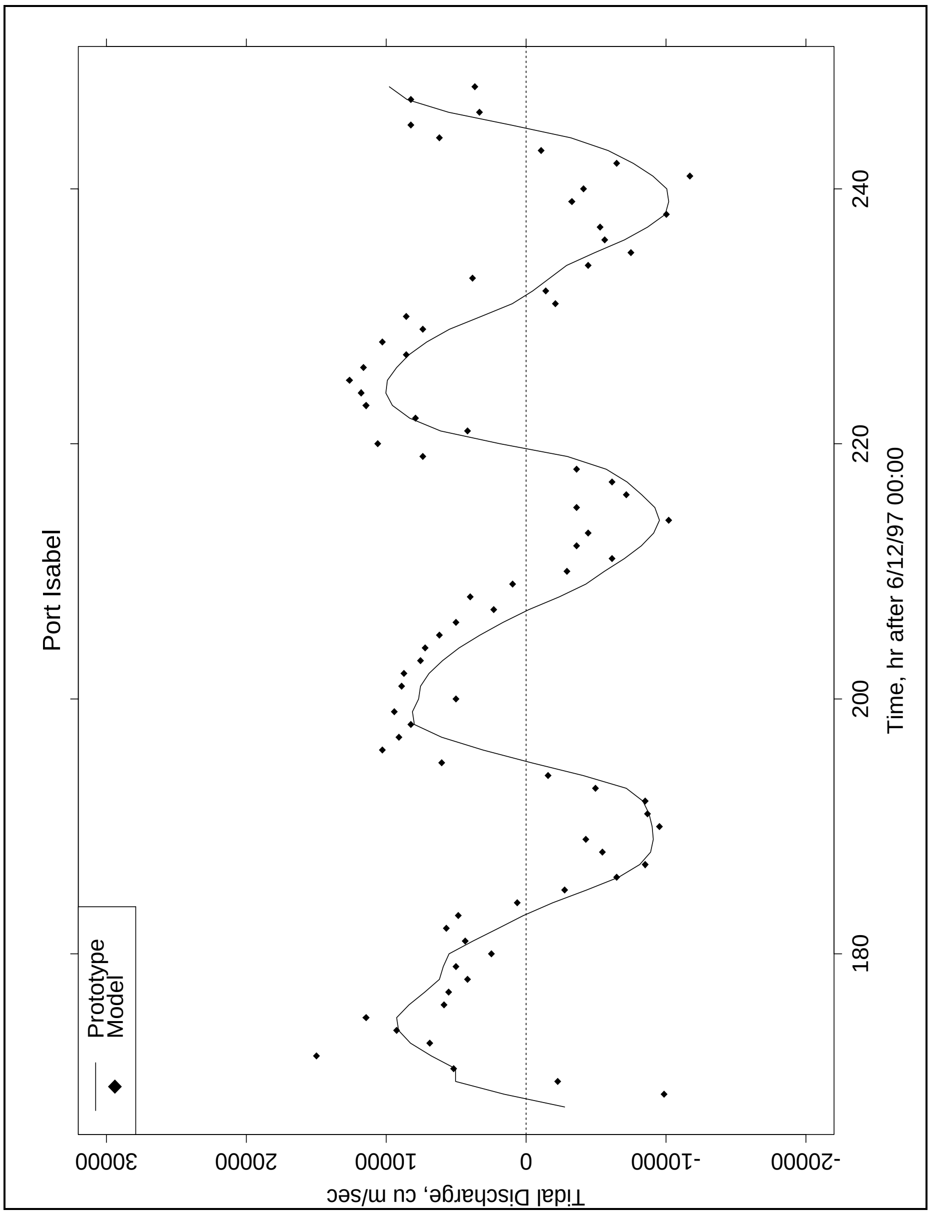

Figure 82. Model and prototype tidal discharges at Port Isabel

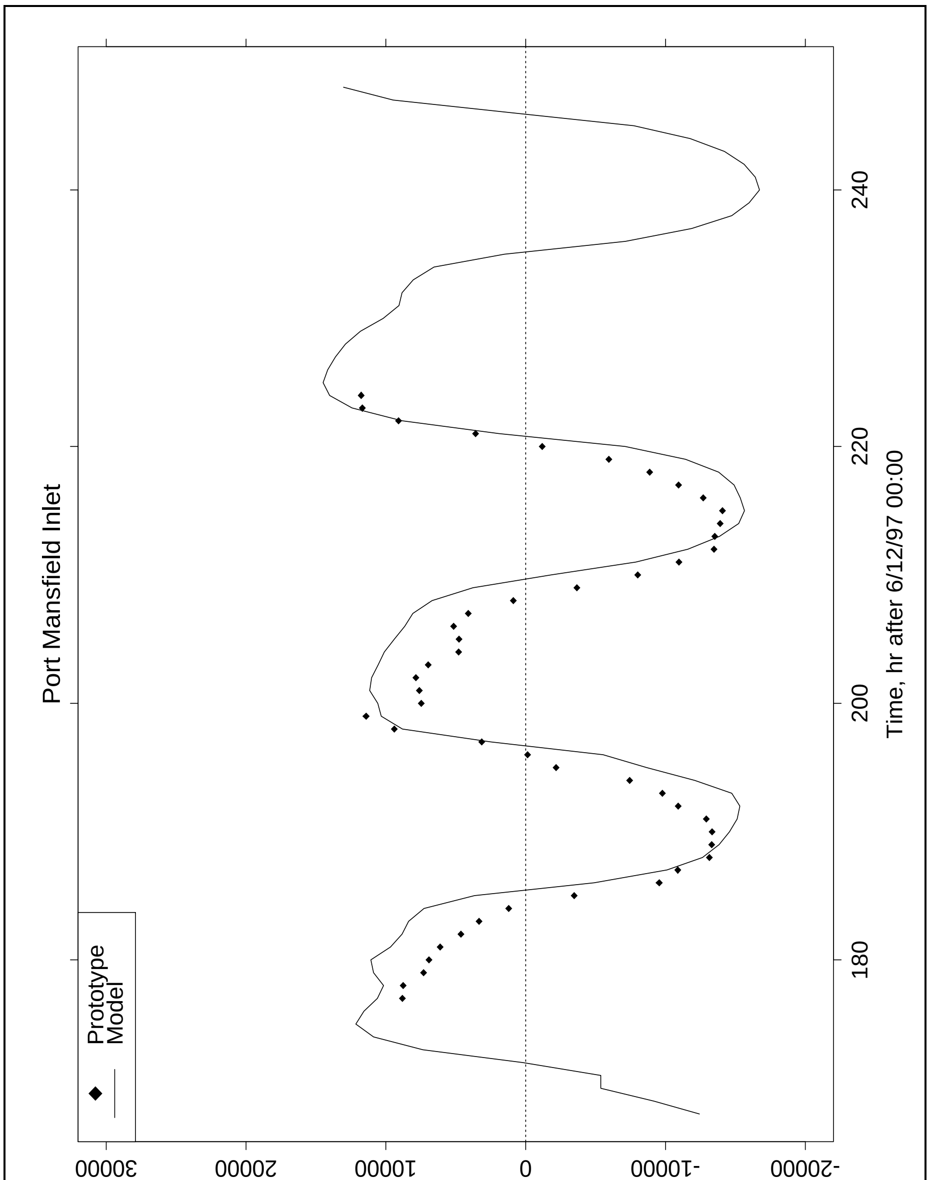

Figure 83. Model and prototype tidal discharges at Port Mansfield Inlet

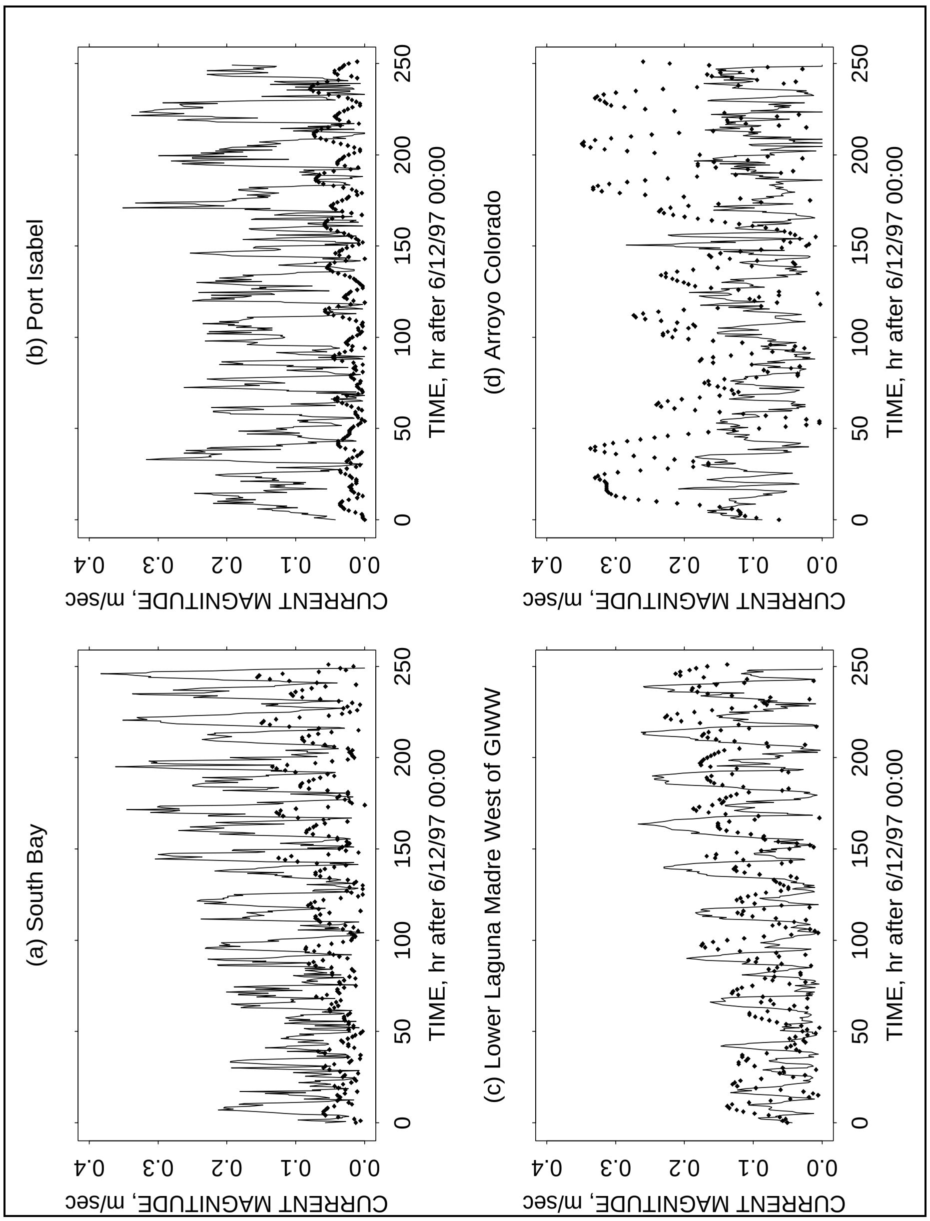

Figure 84. Model versus prototype current magnitudes

suggested that an instrument malfunction was probably responsible for the fact that no positive X-velocity values occurred. Polar plots of field and model data are shown in Figure 85. The model current directions follow depth contour, as expected.

Sediment Transport Model

Four grain classes were specified in the sediment model to represent clay, two silts and fine-sand sized material. The class size intervals were logarithmically spaced. Classes were coupled during erosion and deposition to account for cohesion and the sorting characteristics of fine sediments, as described in Chapter 6. A three-layer bed structure was utilized.

Initial spatial distributions of sediment model grain classes were established by the previous, extensive grain-size measurements of White et al. (1986 and 1989) and by spot measurements made during this study. Grain classes were specified by kilometer-scale areas. The sediment transport model also has a number of parameters which must be adjusted and, unfortunately, few of these can be directly estimated from field observations. Cohesive sediments have transport characteristics which depend on short range electro-chemical forces between particles, and on aggregate configurations. Starting-point transport characteristic values were estimated by laboratory erosion and settling experiments.

Model parameter optimization to validation data sets was an important step in establishing model parameters. The primary validation data sets used in model adjustment were suspended-sediment concentrations, but channel shoaling rates and disposal-area erosion rates were also compared. The TSM data sets were given special importance consistent with the study objects to provide TSM field to the Seagrass Productivity Model.

The validation period for the model was 1 September 1994 through 31 August 1995. Dredging occurred in the prototype, starting about 1 October 1994. Dredging volumes were compiled from Brown and Kraus (1997) and are used here to assemble a disposal scenario for six disposal sites as given in Table 36. The total placed volume was 3.158 million yds^3 (cyds), about 50 percent greater than the average annual dredging in Laguna Madre. The solids content of the disposed material was assumed to be the same as the channel material, about 660 dry-kg/m^3.

The placement in the model was accomplished in seven days and consisted of two parts. Seventy percent of the total material at each site was placed in the bed, and the remaining thirty percent was initially suspended as a plume in the water column within the placement areas. The grain-size distribution of the component parts and total disposed material used by the model were based on WES analyses of channel sediments as given in Table 37.

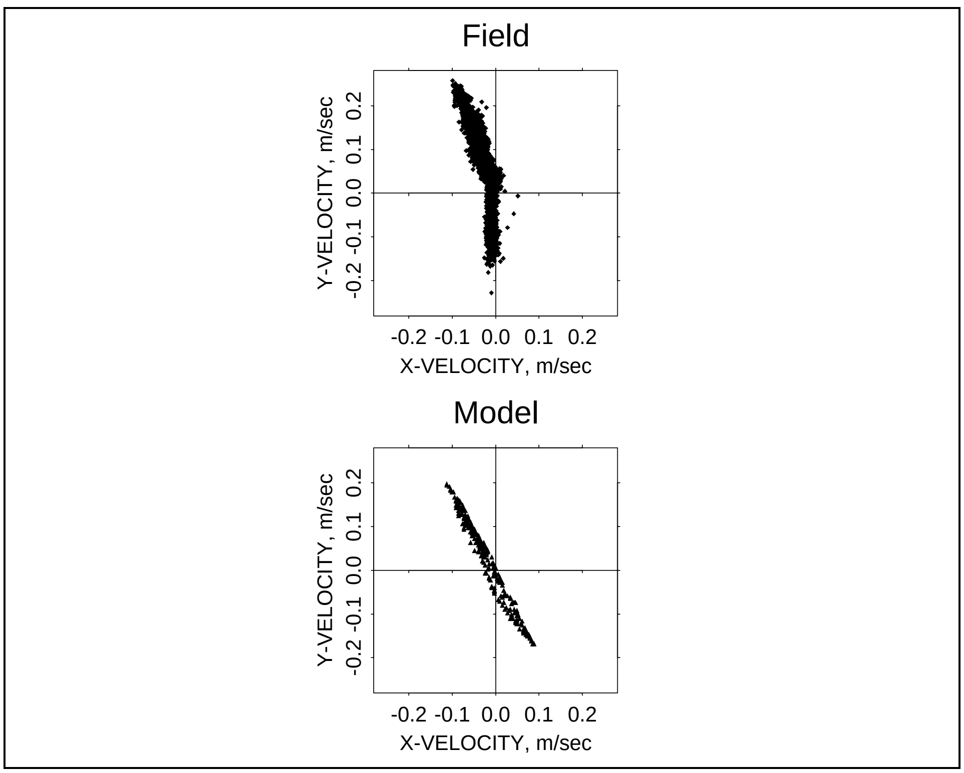

Figure 85. Model and prototype currents West of the GIWW

Table 36 Dredged Material Disposal Characteristics					
CESWG Placement Area	Area, m^2	Disposal volume, cyds	Disposal Rate, dry-kg/m^2	Total Disposal, dry-kg	Placement Thickness, m
187	4.5×10^5	87,250	85	4.38×10^7	0.08
197	5.2×10^5	655,000	414	32.96×10^7	0.50
202	7.8×10^5	512,000	330	25.74×10^7	0.39
211	10.3×10^5	680,000	330	34.09×10^7	0.36
221	12.8×10^5	844,000	330	42.32×10^7	0.34
233	23.0×10^5	380,000	83	19.00×10^7	0.11

Table 37 Grain-Class Distribution for Model Placed Dredged Material				
Placement Fraction	Percent < 4 µm	Percent 4-16 µm	Percent 16-64 µm	Percent > 64 µm
Bed Deposit	22	29	29	21
Suspended Plume	76	17	7	0
Total	38	25	22	15

Validation data sets

Data on TSM concentrations were collected by CBI, the TNRCC, the SPM team, and as described in Chapter 3. LANDSAT Thematic Mapper images were also analyzed to assess correlative TSM distributions over the entire study area at four time instances. Channel shoaling volumes and distributions were compiled by PBS&J (2000) from 50 years of dredging records. Estimates of sediment resuspension and dispersal from select disposal sites were made by Morton (1998).

CBI TSM measurements. Total suspended material (TSM) concentrations were measured at three locations near the PA 233 disposal area in Lower Laguna Madre from September 1994 through August 1995. Samples were collected at 0600 and 1800 hours daily by automatic sampler. These stations were referred to as FIX1 to 3 by Brown and Kraus (1997) and as LLM1 to 3 by Brown (1997). These three stations were located on an east-west line with 1-km spacing, crossing the GIWW about 12 km north from Port Isabel. Station LLM1was located at wave station L1w, shown in Figure 2. All three were located on bare bottom with similar water depths. Further descriptions of these data are given in the next section.

CBI also collected suspended-sediment data in 1995-1996 in the middle of the seagrass area north from Port Isabel and east of the GIWW. This station was designated LLM2a and was located at wave station L2w shown in Figure 2.

Suspended-sediment data for Upper Laguna Madre were omitted from CBI's 1997 report (Militello et al.1997). However, they were obtained from Dr. Adele Militello. She reported that the study team felt there were errors in the data, especially in the first 90 days of the collection period. Apparently, analytical problems resulted in erroneously high TSM values.

TNRCC measurements. The TNRCC has a program of routine water quality monitoring as described in Chapter 3. Laguna Madre monitoring data obtained for this study consisted of quarterly samples from the beginning of 1970 to 1999 collected along the the GIWW by boat. The TNRCC station numbers were in the range of 13443 and 13449. The first two digits were dropped here and prefixed by 'TNR'. These stations are located close to the GIWW as shown in Figures 73 to 75. Station locations are also given in Table 9.

Data from seven TNRCC stations in Laguna Madre were compared statistically to the model results. Because TSM concentrations have been observed to vary strongly with wind conditions, the TNRCC samples are suspected of being biased by boat sampling which necessarily could be made only during moderate weather conditions. Hence, extreme wind conditions and TSM values were probably undersampled. However, these data are deemed to be well suited for the purposes of characterizing normal conditions most important for seagrass.

Model-prototype comparisons

Suspended material. Data from stations LLM1 to 3 covered a relatively small geographic area for one year, with some gaps in records. There were adequate simultaneous data to allow comparisons between stations. Variability in time-series data was conspicuous and indicated that alternate field-model comparisons were needed. Variability could be caused by sampling and analytic errors and/or by variability in environmental conditions, such as wind. Kilometer-scale wind variability is commonly observed in the field but not included in the numerical model, since only a few wind stations are available. Kilometer-scale horizontal-turbulent gyres might also occur in this area as the result of wind stress or water flowing across changing water depths.

A plot of FIX-station TSM values for an example time period is shown in Figure 86. The combined data set, also plotted in Figure 86, was assembled by taking averages of instantaneous values for the three stations, when more than one data were available, or individual values, if not. This combined set included 613 of the possible 730 values. The mean and median values of the instantaneous FIX-station standard deviations, when two or more TSM values were available, were 70 and 34 mg/l for the data shown in Figure 86. For the data set consisting of sample times when all three TSM values were available (265 values of a

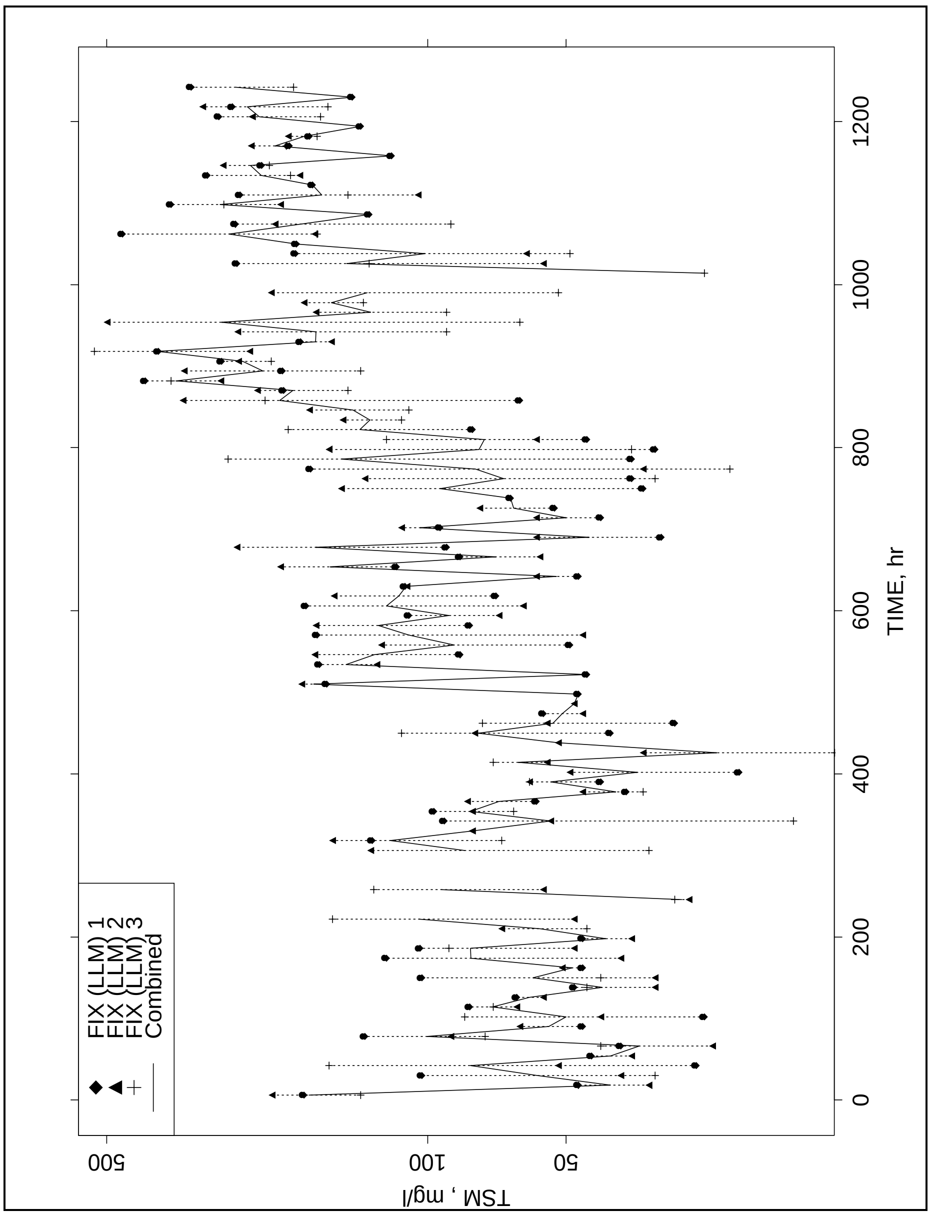

Figure 86. Example TSM data from the beginning of LLM1 to 3 and combined time-series

possible 730) , mean and median values of the instantaneous standard deviations were 70 and 38 mg/l. Instantaneous standard deviations among stations were log-normally distributed.

Statistical comparisons of simultaneous LLM1 to 3 and combined data (265 values of a possible 730) are presented in Table 38.

Table 38
Statistical Analyses of LLM1 to 3 and Combined Data Sets

		Test Matrix		
Statistic	Station	LLM2	LLM3	Combined
Paired t-Test: Mean Differences, mg/l * mean differences not equal to zero (p-value<0.05)	LLM1	21.4 *	46.4 *	22.6 *
	LLM2		25.0 *	1.2
	LLM3			-23.8 *
Variance Test: 95% CI Ratio of Variances * true ratio not equal to one	LLM1	0.81 - 1.31	1.36 - 2.21*	1.3 - 2.11 *
	LLM2		1.33 - 2.15 *	1.27 - 2.06 *
	LLM3			0.75 - 1.22
Correlation Coefficient (R): trim=0 (trim=0.05)	LLM1	0.51 (0.67)	0.54 (0.67)	0.82 (0.88)
	LLM2		0.71 (0.84)	0.87 (0.90)
	LLM3			0.86 (0.90)

Analyses indicated that TSM values were progressively less from west to east by 21 and 46 mg/l for LLM1 to 3. This trend could reflect a source of resuspension west of the channel such as the high-turbidity bare area shown in Figure 34 and 35 or resuspension from the PA 233. Variances at LLM1 and 2 were significantly greater than at LLM3 or the combined data set. The combined TSM data set was most like the LLM2 data set in mean value and most like station LLM3 in variance. Correlation coefficients are sensitive to extreme differences and the fraction trimmed from positive and negative ends of distributions.

Comparison of field and model data were made by use of corresponding statistical distributions. This method is attractive here because of the nature of the field data and because the TSM or underwater light conditions important to seagrass are not sensitive to timing or extreme values. Cumulative frequency distributions constructed as standard normal/deviation from the median for LLM1 to 3 and combined data sets are shown in Figure 87. Standard normal coordinates correspond to percentile frequency of occurrence. For example, -2, -1, 1, and 2 quantiles of the standard normal correspond to 2, 16, 84, and 98 percentiles. The ordinate of Figure 87 is a logarithmic scale since these distributions are much closer to log-normal than to normal.

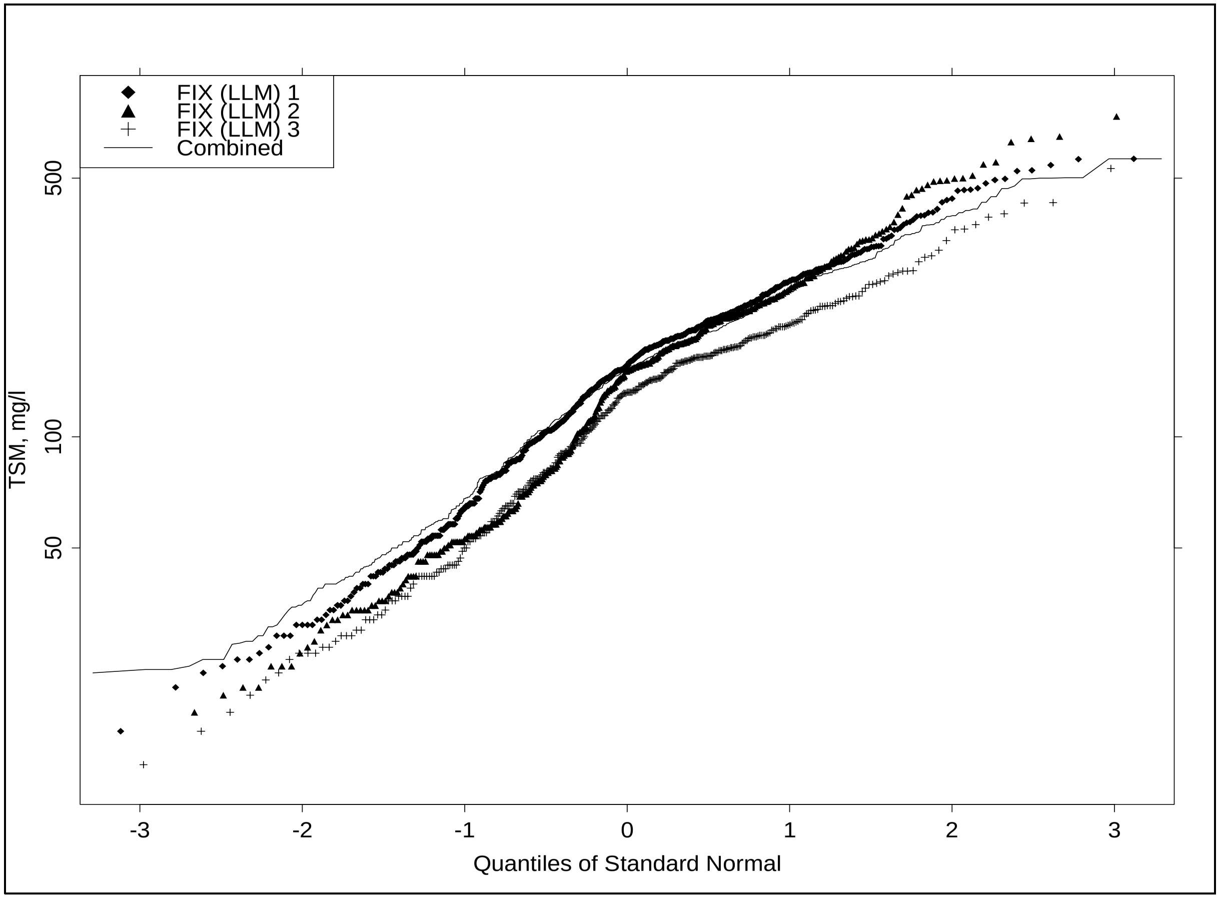

Figure 87. Cumulative standard-normal distributions for LLM1 to 3 and combined data sets (see text for further explanation)

The model validation included seven stations monitored by the TNRCC. Time-series TSM values for the four stations in Lower Laguna Madre are shown in Figure 88. As can be seen in Figure 88, variability between stations at a given instant in time is appreciable. A plot of the statistical distributions of these four stations is shown in Figure 89. Like the CBI stations, the TNRCC TSM data are log-normally distributed.

Table 39 contains model-to-prototype comparisons made for the validation of model TSMs. TNRCC stations are arranged north to south in the table. Also included in the table are CBI stations in the bare area near PA 233 (FIX1 or LLM1) and in seagrass (LLM2a). The GIWW channel and channel side-slopes are described in the model with material types. Model adjustment was therefore limited to global sediment parameters. Values of total suspended material (TSM) at 15, 50, and 85 percentile levels were determined and are presented in Table 39. Plots of model and prototype TSM time-series at LLM1 are shown in Figure 90.

Table 39
Model Validation TSM Comparisons

	TSM, mg/l					
	Field			Model		
Station	15 %	50 %	85 %	15 %	50 %	85 %
TNR-443	8	26	56	3	18	89
TNR-445	11	25	51	8	14	42
TNR-444	15	34	81	14	31	75
TNR-449	12	24	60	15	47	130
TNR-448	16	27	54	5	12	32
TNR-447	15	30	60	2	9	47
TNR-446	13	30	61	7	23	62
CBI-FIX [1]	65	150	253	58	122	258
CBI-LLM2a [2]	11	15	28	9	14	24

[1] From with-disposal scenario
[2] From no-disposal scenario

Dispersion of sediment from PAs. The percent of material resuspended from the placement areas was calculated at the end of the year-long model simulation. Results are presented in Table 40 along with dispersion rates estimated from field information.

Total loss from the placement areas was 43.7×10^7 dry-kg or about 28 percent of the overall disposed mass. This magnitude of sediment loss converts to a channel-shoal volume of about 8.71×10^5 cyds.

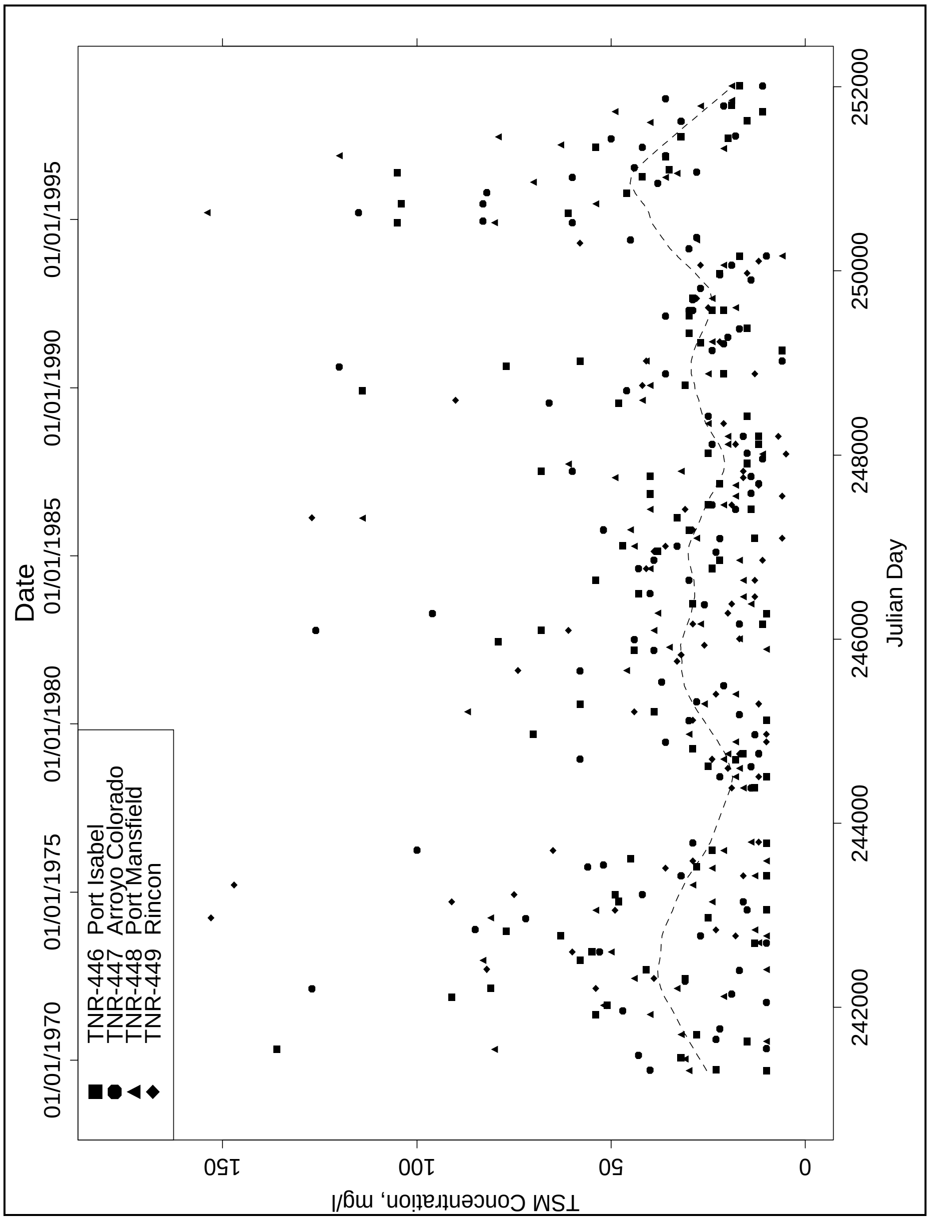

Figure 88. Lower Laguna Madre TNRCC station TSM time-series

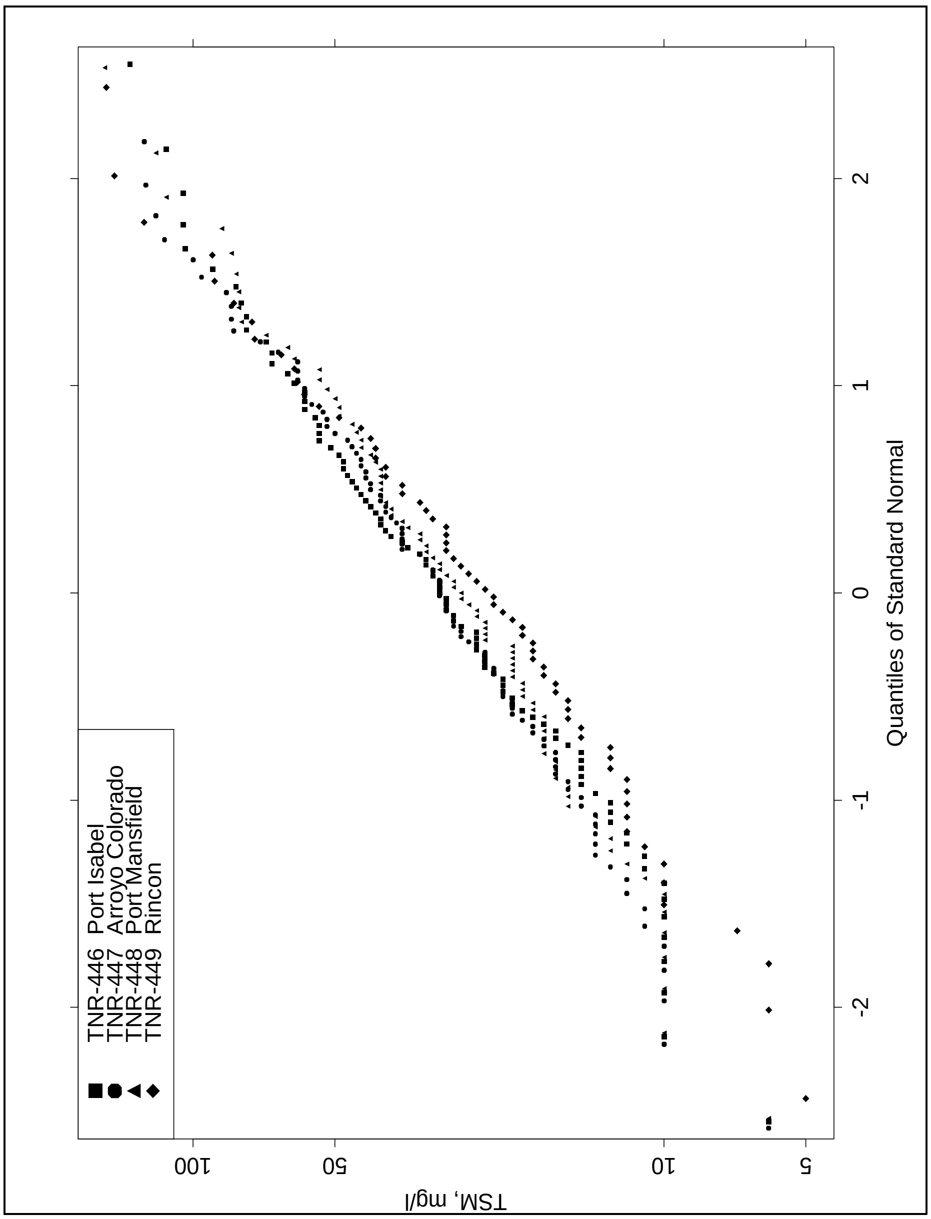

Figure 89. Cumulative standard-normal distributions for Lower Laguna Madre TNRCC stations

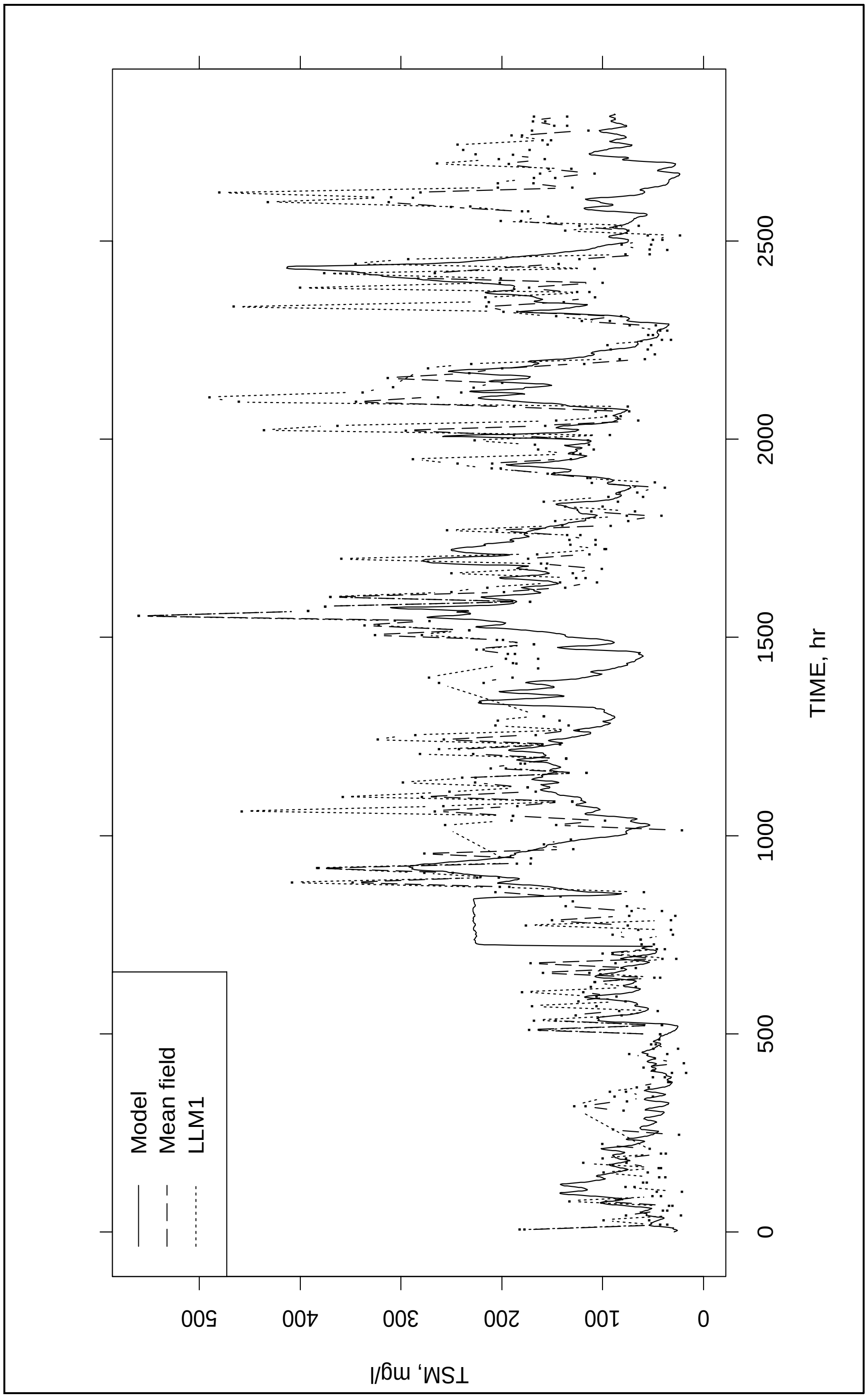

Figure 90. Example model and prototype TSM time-series at LLM1 starting 1 September 1994. Disposal occurred during hours 720 to 840

Table 40
Model Sediment Dispersion from Disposal PA

CESWG Placement Area	Total Disposal, dry-kg	Percent Lost by Erosion and Transport	
		Model	Field[1]
187	4.38×10^7	23.3	48.1
197	33.0×10^7	30.5	70.5
202	25.7×10^7	28.8	54.6
211	34.1×10^7	19.4	34.5
221	42.3×10^7	24.7	1.5
233	19.0×10^7	42.7	94.6

[1] Morton (1998)

Channel shoaling. Sedimentation model results were used to estimate the effect of in-bay disposal on channel shoaling. The model was not adjusted for channel shoaling volumes or distributions, nor is the channel well resolved by the mesh (only one element wide), but the properties of the channel material are identical to the sediment properties of disposed material. The model was adjusted to sediment conditions in Laguna Madre, and not specifically to sediment conditions in the channels.

Information on deposit heights and sediment masses were extracted from model results at nodes located along the channel. The main GIWW channel reach was taken to begin just inside Brazos Santiago Pass, run the lengths of Lower and Upper Laguna Madre, the Land Cut, and terminate at the junction with Corpus Christi Bay. Along the main GIWW reach, 1980 nodes along both edges of the channel were extracted. The distance along the channel was calculated from the nodal locations, and the change in bed elevation (*delbed*) was plotted in raw and smoothed forms. The smoothed curve was used to approximate *delbed*'s at 200-m intervals over the main GIWW reach. The trapezoidal rule was used to integrate positive *delbed*'s over the respective reaches to estimate shoal areas, which were multiplied by channel width to obtain the shoaling volume. The channel shoaling values were not adjusted or scaled in any way.

Since the model was not specifically validated for channel shoaling, two sets of model results were analyzed as a sensitivity-testing of the disposal effect on channel shoaling. The channel deposit thicknesses for the validation sediment model run is shown in Figure 91. The locations of the six placement sites are shown there. The model displayed highest channel shoaling near the location of PA 233 and the area of cross-channel currents described earlier. An additional model run with less channel shoaling, referred to as the sensitivity run, was also analyzed. Shoaling distribution for this model run was vary similar to the validation model run. Channel shoaling was calculated from both six-disposal scenarios and matching without-disposal runs. Results are presented in Table 41.

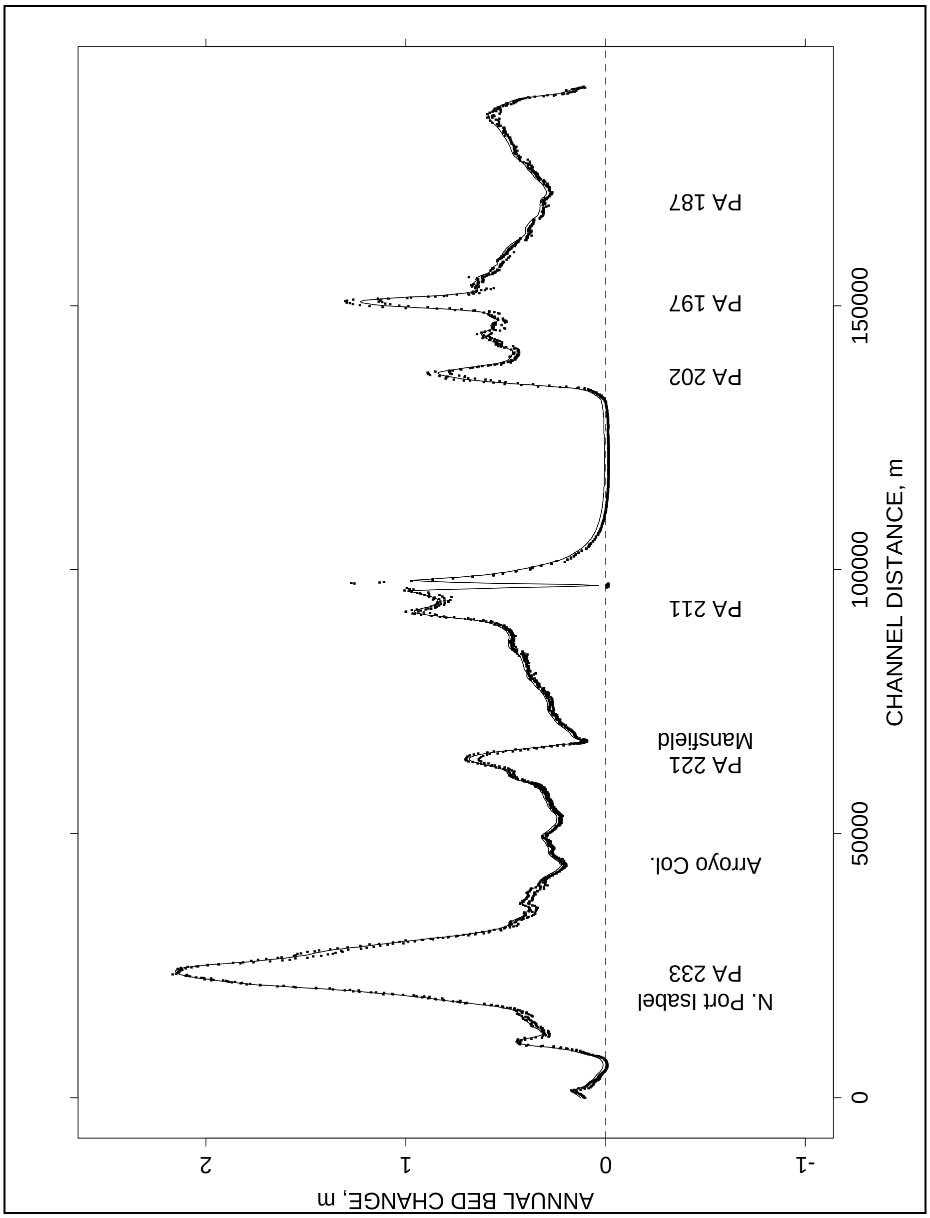

Figure 91. Channel shoaling distribution for validation model run

Table 41
Example With- and Without-Disposal Model Channel Shoaling Volumes

Model Run	No-Disposal Shoaling, m^3	Shoaling with Disposal, m^3	Percent Decrease	Decrease as Percent of Dispersed
Validation	3.04×10^6	3.22×10^6	5.6	20.6
Sensitivity	3.13×10^5	3.70×10^5	15.4	6

As described in Chapter 1, the mean annual shoaling rate is about 1.6×10^6 m^3 over the 50-yr history of the channel. Therefore, the validation model run produced channel shoaling about twice the actual value. The sensitivity model run produced channel shoaling about one-tenth that of the validation run. Eliminating in-bay disposal and associated sediment dispersion from six placement sites would decrease channel shoaling by about 11 percent in the main GIWW reach, according to an average of these runs. About 14 percent of the dispersed sediment is expected to return to and be captured by the main GIWW channel.

Base Simulations

The hydrodynamic and sediment transport model of Laguna Madre was used to perform base annual simulations of sediment resuspension with and without dredged material disposal for a scenario based on existing placement areas (PA). Output was extracted from the model at certain locations and used to drive the seagrass productivity model (SPM) of the Laguna developed by the University of Texas and Texas A&M seagrass modeling team. The purpose of the model simulations was to provide realistic suspended-sediment time-series, especially within the seagrass areas where the SPM stations were located. In addition, the model results were processed and displayed here to gauge water column and seagrass light-availability impacts in the proximity of the six placement areas included in the disposal scenario.

Scenario description

A worst-case dredged material placement scenario was simulated with simultaneous disposal at three sites in Upper Laguna Madre and three sites in Lower Laguna Madre. The placement characteristics were the same as for the validation period presented in Table 36, except that the disposal was specified to occur in April to have the greatest impact on seagrass at the beginning of their growth season.

The placement was simulated to occur on 1 April 1995. The bed placement was accomplished in 24 simulated hours in the model. The suspended plume was formed as a constant flux into the water column over 119 hours, or roughly 5 days starting 1 April 1995. The simulation continued until 1 September 1995 and then wrapped back to 1 September 1994 and continued until 1 April 1995 for a total simulation time of one year.

Based on field observations near a pipeline discharge, reported in Chapter 5, and ICT review comments, the sediment and disposed material characteristics were changed slightly from the validation simulations. Tidal and wind-driven currents were calculated, combined with wind-wave shear stresses, and used to calculate sediment erosion, deposition, and transport for the simulation period of one year. Scenarios with and without dredged material placement were simulated.

Results

Model results were compiled for TSM, channel shoaling, and PA sediment dispersion since sediment parameters and the disposal scenario were changed from the validation model runs. Comparison of TSM values are presented in Table 42.

Table 42
Model Base-Simulation TSM Comparisons

	TSM, mg/l					
	Field			Model		
Station	15 %	50 %	85 %	15 %	50 %	85 %
TNR-443	8	26	56	6	29	99
TNR-445	11	25	51	8	28	60
TNR-444	15	34	81	21	47	89
TNR-449	12	24	60	24	60	116
TNR-448	16	27	54	11	24	51
TNR-447	15	30	60	5	25	87
TNR-446	13	30	61	10	21	45
CBI-FIX1	65	150	253	[1] 63	91	126
				[2] 59	84	117
CBI-LLM2a	11	15	28	[1] 15	18	27
				[2] 15	18	26

[1] From with-disposal scenario
[2] From no-disposal scenario

The sediment dispersion from the PAs are given in Table 43. PA sediment dispersion increased over the validation simulations but were closer to typical prototype conditions (see Table 40).

Table 43
Base-Run Model Sediment Dispersion from Disposal PAs

CESWG Placement Area	Total Disposal, dry-kg	Percent Lost by Erosion and Transport
187	4.38×10^7	25.3
197	33.0×10^7	40.0
202	25.7×10^7	39.5
211	34.1×10^7	25.2
221	42.3×10^7	32.1
233	19.0×10^7	83.0

Model channel shoaling along the length of the GIWW was 3.00×10^6 m^3 (3.92×10^6 cyds) without disposal and 3.20×10^6 m^3 (4.18×10^6 cyds) with disposal. Model channel shoaling volume (and distribution) was about the same as for the validation model run.

Water column impacts

Model results and comparisons are presented in Appendix B. Average TSMs were calculated for the period of the plume release and shown in Plates B1 and B2. During this period, currents carried the plume outside the limits of the placement areas in some cases. In these and other figures, 5,000-m north-south/east-west grid lines or grid points are shown. The average TSM for the remaining 597 hours of April 1995 after the placement are shown in Plates B3 and B4. Monthly-average TSM plots for May through March are shown in Plates B5 to B26.

Model results were used to calculate the increase in total suspended sediment resulting from the placement of the dredged material and its subsequent resuspension from the placement areas. Average disposal effects were estimated for the period of the plume release and shown in Plates B27 to B29. The average post-placement TSM differences for the remaining 597 hours of April 1995 are shown in Plates B30 to B32. Monthly-average TSM difference plots for May through March are shown in Plates B33 to B64.

Light availability effects

The SPM model team determined a relationship between total suspended sediment (TSS) and the diffuse attenuation coefficient K_d for photo-active radiation, as given in Equation 33. Seagrass requires about 20 percent of the surface irradiance Q_o to survive long-term. The irradiance reaching the seagrass depends on the water depth h and K_d, as given in Equation 31. Combining these equations for use in the model post-processing system yielded:

$$\ln\left(\frac{Q}{Q_o}\right) = -((196.1226 + 637.48\,TSS)^{0.5} - 13.9) * h \;/\; 0.31874 \qquad (69)$$

where the TSS is the monthly average in kg/m^3 and h is in m. Note that the TSS value used for this calculation was the mean for the respective month, and since the distribution of TSS is quasi-lognormal, the means are higher than the medians and skewed toward the upper end of the distributions. The conversion of $ln(Q/Q_o)$ to percentiles reaching the bed is described in Table 44.

Table 44
Example Irradiance Percentages and $ln(Q/Q_o)$ Reaching the Bed

Percentile of Irradiance Reaching the Bed (Q/Q_o x 100)	$ln(Q/Q_o)$
50	-0.69
30	-1.204
20	-1.609
10	-2.303

As stated earlier, the critical value for seagrass survival is about 20 percent irradiance reaching the bottom. The 20-percent bottom irradiance contours for both during-disposal and non-disposal scenarios are shown in Plates B65 to B67. The disposal scenario contour lines shown are thin, and the non-disposal lines are thick. The thick line eclipses the thin line, so that if only a thick line shows in a figure, there was no difference between the two. The monthly 20-percent bottom irradiance contours for disposal and non-disposal scenarios are shown in Plates B68 to B103. There was no divergence of contour lines in the vicinity of PA 187.